VLF-EM study for archaeological investigation of the labyrinth mortuary temple complex at Hawara area, Egypt

Article *in* Near Surface Geophysics · June 2010

DOI: 10.3997/1873-0604.2010004

Mohamed Khalil
Montana Tech of the University of Montana

Abbas Ali
National Research Institute of Astronomy and Geophysics

Hany Mesbah
National Research Institute of Astronomy and Geophysics

Usama Massoud
National Research Institute of Astronomy and Geophysics

Near Surface Geophysics, 2010, **8**, 203-212 doi:10.3997/1873-0604.2010004

VLF-EM study for archaeological investigation of the labyrinth mortuary temple complex at Hawara area, Egypt

Mohamed Ahmed Khalil[1,2], Abbas Mohamed Abbas[1*],
Fernando A. Monteiro Santos[2], Hany S.A. Mesbah[1] and Usama Massoud[1]

[1] *National Research Institute of Astronomy and Geophysics (NRIAG), 11421 Helwan, Cairo, Egypt*
[2] *University of Lisbon, Centro de Geofísica da Universidade de Lisboa – IDL, Campo Grande, Ed. C8, 1749-016 Lisbon, Portugal*

Received July 2008, revision accepted January 2010

ABSTRACT
The present study is a test of the applicability of the VLF-EM method in archaeological prospecting. The Hawara area is about 90 km south of Cairo and is the location of an important archaeological site known as the labyrinth mortuary temple complex, situated south of the Hawara pyramid. No official excavations have been carried out in the labyrinth complex since 1911. VLF-EM was employed in this study using a small grid, 2 m between profiles and stations. The measured data were interpreted using Fraser and Karous-Hjelt filters. Two-dimensional (2D) resistivity cross-sections have been calculated inverting VLF-EM data in a quantitative manner. A three-dimensional (3D) resistivity inversion scheme has been applied to a grid of nine Schlumberger vertical electrical soundings to provide information on the resistivity of the shallow and deep structures in the study area. Results show a large group of elongated and square subsurface anomalies at shallow depths, connected in some parts and separated in others. The spatial distribution of the anomalies significantly matches a historical description by Herodotus.

INTRODUCTION

The pyramids of Egypt are arguably the most famous archaeological structures in the world. The majority of pyramids date to the Old Kingdom (2613–2181 BC) and most attention has been focused on limestone pyramids, such as those at Giza. However, the method of construction later changed; rather than being built entirely of limestone, pyramids were built with a mud-brick core and an outer casing of limestone. One of the most important of these mud-brick structures is the Dynasty XII funerary complex of King Amenemhet III, which was started at Hawara around 1840 BC, in the 15th year of his reign (Keatings *et al.* 2007). Nowadays, the pyramid is little more than an eroded, vaguely pyramidal mountain of mud brick (Fig. 1). From the once magnificent mortuary temple precinct, formerly enclosed by a wall, there is little left beyond the foundation bed of compacted sand, chips and shards of limestone.

The pyramid complex is located on the northwestern edge of the Hawara Channel and is built over an outcropping limestone rock base at an altitude of ca. 32 m above sea level. It commands a prominent position overlooking the Hawara Channel and, to the west, faces the agricultural expanse of the Faiyum depression (Brown 1892; Butzer 1976).

The Hawara Pyramid enclosure is perhaps best known for the labyrinth mortuary temple complex situated between the pyramid and the causeway that entered the enclosure at its south-east corner. In Late Antiquity, the complex was considered as one of the wonders of the world. The mortuary temple has been described by classical authors, such as Herodotus (II, 148–9), Strabo (17. I. 3, 37, 42) and Pliny (Natural History 36, 13) as having twelve main courts surrounded by rooms, galleries and more courtyards. Herodotus claimed there were 3000 rooms in all (Armayor 1985). Strabo (ca. 64 BC–19 AD) praised it as a wonder of the world. He

FIGURE 1
The pyramid of Amenemhet III at Hawara.

* dr.abbas.ali@gmail.com

described the labyrinth as having hidden chambers that "are long and large in number and have paths running through one another which twist and turn, so that no one can enter or leave any court without a guide. And the wonder of it is the roofs of each chambers are made of single stones". Since Ptolemaic times, especially under the Romans, the complex was used as a quarry and hence has mostly disappeared (Lloyd 1970).

The location of the labyrinth has been described by many expeditions. The French expedition (1799–1800) described the Hawara pyramid and the pharaonic temple south of it. The northern and western remains were wrongly identified as the labyrinth (Jomard and Caristie 1822). Petrie (1912) mentioned also that on the south of the pyramid lay a wide mass of chips and fragments of building material, which had long generally been identified with the celebrated labyrinth. Petrie depicted partial reconstructions of the complex to the south of the pyramid (Fig. 2b).

Around 1840, the original labyrinth site at Hawara was rediscovered by the Prussian expedition of Richard Lepsius (1849). He carried out considerable excavations in the cemetery to the north, on the northern and south-eastern sides of the pyramid and in the area of the labyrinth and claimed to have established the actual site of the labyrinth. Lepsius (1849) thought that the structures excavated by his team were parts of the temple of King Amenemhat III but later research showed that they belonged to Roman tombs, where in Ptolemaic times, especially under the Romans, the complex was used as a quarry (Lloyd 1970).

Since the expedition of Richard Lepsius, the place came to be known as a location to find high quality royal statues. In 1888, Flinders Petrie started to excavate at Hawara, north of the pyramid. The results of his work on the labyrinth itself were disappointing for him. Since Roman times the whole building had been totally destroyed and he was unable to recover any part of the complex. Sensationally though, he found a series of portrait panel paintings, depicting the local elite in the period of Roman rule (Petrie 1889, 1890). With these findings, he restored to classical art history a field that had been virtually unknown until then.

In 1911, Petrie returned to Hawara to excavate in the labyrinth and to find more of the so-called Faiyum portraits on the Roman period mummies.

The scholar Athanasius Kircher (1602–1680) produced one of the first pictorial reconstructions (Fig. 2a), mainly based on the account by Herodotus. At the centre of his architecture drawing, Kircher placed a maze, most likely to have been inspired by Roman labyrinth mosaics and surrounded it with the twelve courts described by Herodotus (Kern 1995).

Petrie *et al.* (1912) also depicted partial reconstructions of the complex within his volumes (Fig. 2b). It consists of 18 large chambers separated by three main corridors, two running sideways and one at the centre. Because he did not find enough evidence, these are considered to be primarily based on the classical authors and only a few points depended on the little evidence he found for the original architecture. The structure is simpler than the one that Herodotus (II, 148–9), Strabo (17. I. 3, 37, 42) and Pliny (Natural History 36, 13) described.

The dimensions of the labyrinth mortuary temple complex are approximately 120 m by 300 m (Arnold 1979). He assumed that the building followed the tradition of the Djoser complex in Saqqara. There is no available information concerning the burial depth of the labyrinth.

Since Petrie's excavations in 1911, no official excavation has been carried out in the labyrinth, though some shorter expedi-

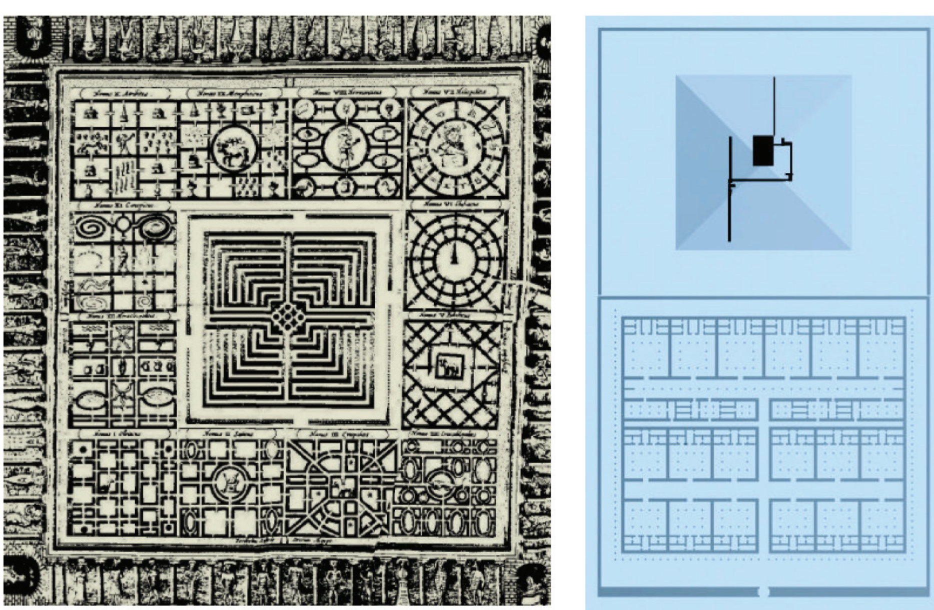

(a) (b)

FIGURE 2
a) Egyptian labyrinth. Athanasius, Kircher (1602–1680), from Kern (1995). b) Schematic diagram of the expected labyrinth mortuary temple complex (after Petrie *et al.* 1912).

tions from the Antiquity Service have dug in the Necropolis of Hawara. The main object of the present study is to contribute to the test of the historical legend about the shape and structure of this labyrinth.

GEOLOGICAL SETTING

The Hawara area is located about 90 km south of Cairo in the Hawara Channel (Fig. 3). It resembles a lowland passage that connects the fertile Faiyum depression with the Nile Valley. The Hawara Channel has been highly modified hydrologically. It is a key point in the landscape of Middle Egypt; through it, Nile water flows through the Bahr Yussef and Bahr Wasif canals into the Faiyum depression. As noted in the introduction, the pyramid complex is situated on the northwestern edge of the Hawara Channel and is built on an outcropping limestone rock base at an altitude of ca. 32 m a.s.l. It commands a prominent position overlooking the Hawara Channel and, to the west, faces the agricultural expanse of the Faiyum depression (Keatings *et al.* 2007).

According to the stratigraphic classification of Swedan (1986), the subsurface stratigraphic column is capped by Quaternary deposits, which have a very wide distribution over the whole area of El-Fayum. It is composed of sands, gravels, limestone pebbles, silt, clay and gypsum. They originate from alternating sedimentation and erosion during the Pleistocene, continuing into the Holocene. They directly overly the limestone rocks of the Middle Eocene, where the latter are extended to a greater depth. The depositional environments and sequence succession of the underlying limestone resulted in the accumulation of thick Quaternary deposits in this region (Swedan 1986).

At the same time, Middle Eocene limestones and marls (Mokattam Formation) outcrop in the area as isolated patches and one of them forms the base of the pyramid. Middle Eocene rocks are in contact with Quaternary deposits, separated by a probable fault (Fig. 3).

Figure 4 shows two soil-cores to the south of the Hawara pyramid (B1 and B2), reaching 15 m depth and showing the shallow Quaternary deposits.

GEOPHYSICAL DATA ACQUISITION

There are many studies concerned with the application of different geophysical methods for discovering hidden archaeological structures in different geographic locations. Bozzo *et al.* (1999) used VLF-EM to highlight some archaeological structures characterized by different conductivities at depths shallower than 4–5 m in the eastern hill of the Selinunte archaeological site, on the south coast of Sicily. Mahmut (2006) used an integrated geophysical investigation, including magnetics, 2D resistivity, VLF-R and seismic methods to determine the buried archaeological structures under the very thick soil in the upper part of the Sardis archaeological site, Turkey. Papadopoulos *et al.* (2007) implemented a simple modification of a standard resistance-meter geophysical instrument, in order to collect parallel two-dimen-

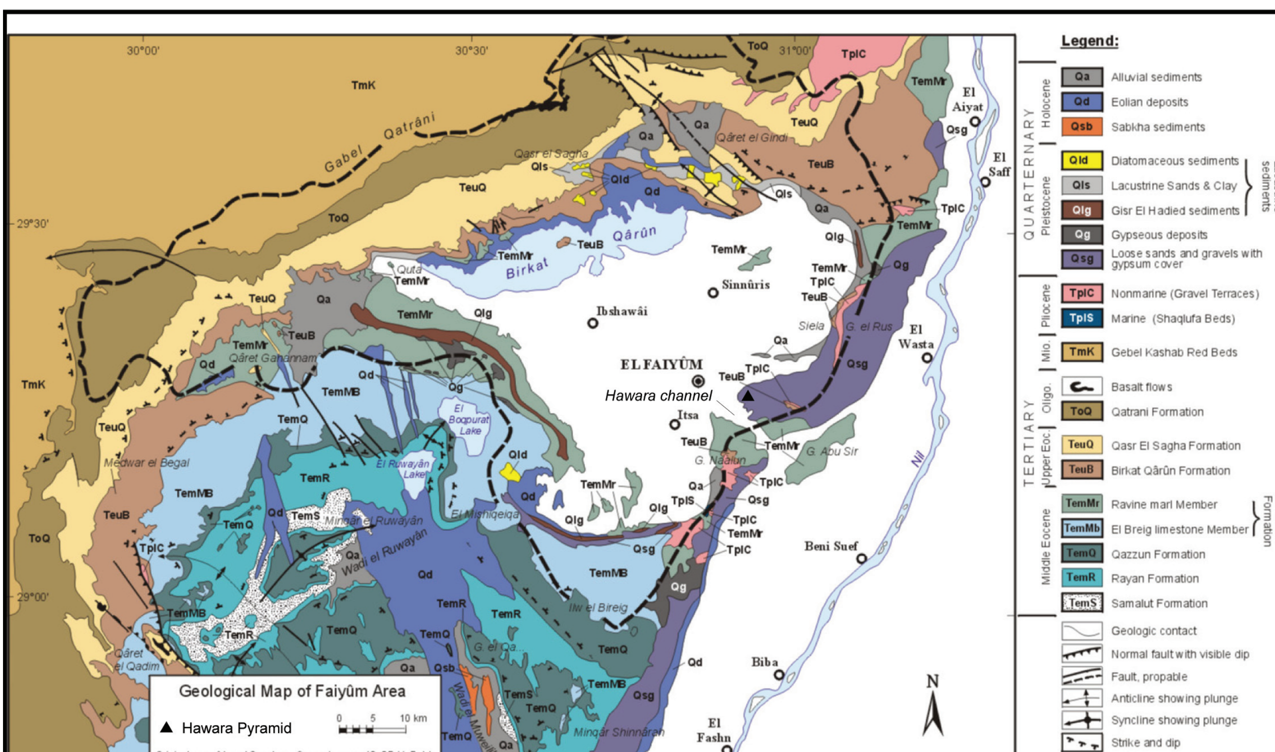

FIGURE 3
Geological map of the Faiyum area (after Swedan 1986).

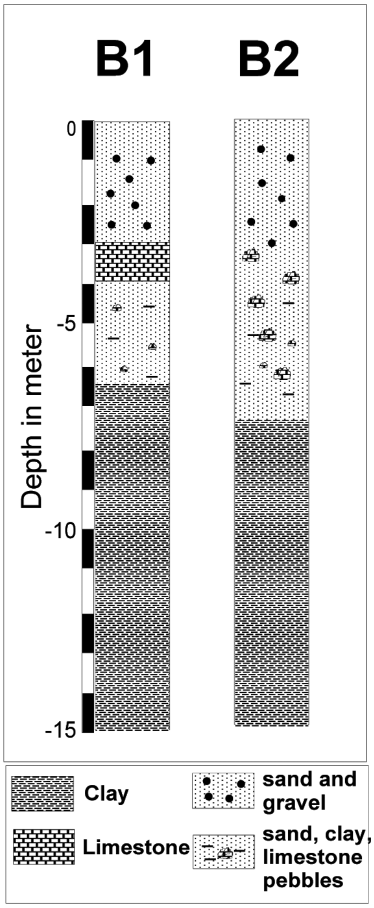

FIGURE 4
Soil-cores B1 and B2, south Hawara Pyramid. (After ministry of irrigation, El-Fayum governorate, pers. comm.)

sional sections along the *X*-, *Y*- or *XY*-direction in a relatively short time, employing a pole-pole array in archaeological sites.

In the present study, two geophysical methods were applied; vertical electrical soundings (VES) and very low frequency electromagnetic method (VLF-EM). Since we have no detailed stratigraphic description of the study area, we used vertical electrical soundings (VES) for both reconnaissances of the general subsurface geoelectric succession and to use the average resistivity value of the media during the two-dimensional VLF-EM inversion later on.

The predictable resistivity dissimilarity between resistive Pleistocene deposits – sands and gravel – and conductive archaeological units in the labyrinth mortuary temple complex – mudbrick (Keatings *et al.* 2007) is the key tool for archaeological prospecting by the VLF-electromagnetic method. We used the VLF-EM method in the present study to check the capability of this technique for archaeological prospecting in relatively small-scale conductive and complex structures as buried walls of the temple, since it has been long used in groundwater exploration in saturated and conductive large-scale fractured zones along wades.

The electrical survey was conducted using a Syscal R2 device. Nine vertical electrical soundings were measured in the study area using a Schlumberger array, forming a somewhat regular grid (Fig. 5). The AB/2 distance ranges from 1–400 m in some stations. The direction of array in all stations is north-south. The VLF survey covers an area of 100 m × 140 m to the south of the Hawara pyramid, in the area where we expected to find the labyrinth structure. The electromagnetic survey was carried out using an ABEM WADI VLF device. We measured seventy five parallel VLF-EM profiles; each profile extends roughly NNW-SSE. The majority of the VLF-EM profiles have a total length of 100 m. The transmitter frequency was 18.1 kHz, which corresponds to a

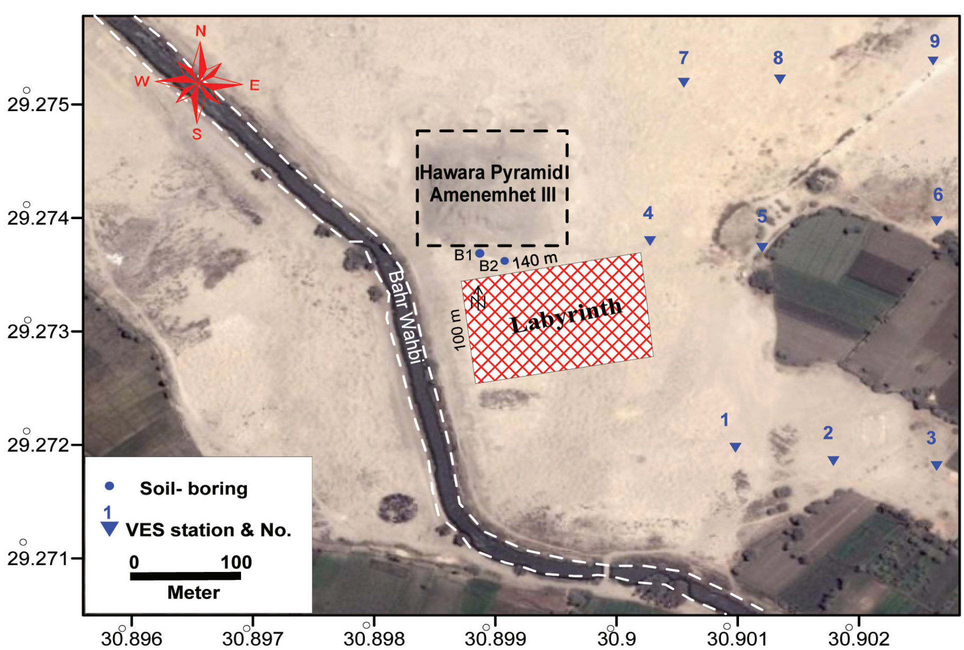

FIGURE 5
Location map of Hawara pyramid, VLF and VES survey areas.

Russian transmitter. The distance between profiles and stations is two metres respectively in order to have a regular and condensed spatial distribution of data points. Vertical electrical soundings were conducted very close to the VLF surveyed area (expected labyrinth structure) but not in the same location, since VES may be destructive to the archaeological site.

VERTICAL ELECTRICAL SOUNDINGS

A code for 3D resistivity modelling and inversion of vertical electrical soundings proposed by Monteiro Santos and Sultan (2008) is applied upon the measured nine Schlumberger vertical electrical soundings. The 3D resistivity code is based on the finite element technique and regularization method. A detailed description of the method and the code is found in their paper.

The mesh used for forward calculation of each sounding consists of 34 × 37 × 35 nodes. Both meshes have been defined after trials and according to the AB/2 values and site spacing. A 20 Ωm uniform medium was taken as the initial model. After some tries, the initial value of the Lagrange parameter (or damping factor) was chosen as 0.4. The results are presented in Fig. 6 as horizontal slices of the resistivity model. This model was obtained after 10 iterations. The model response approaches the field data within the limits of data errors.

GEOLOGICAL INTERPRETATION OF THE VERTICAL ELECTRICAL SOUNDINGS

The resulted 3D model shows that the southwestern half of the area is covered by a shallow high resistive layer and that the resistivity gradually decreases to intermediate values at 7.5 m deep. This layer may correspond to the dry surface layer of Pleistocene sands, gravels and limestone pebbles (see Fig. 4). It is underlain by a low resistivity layer to a depth of about 60 m in its northeastern part. This low resistivity layer may be corresponding to a succession of different geologic beds, characterized by highly conductive materials and combining in one single geoelectric layer. According to the geologic succession, such conductive geologic beds are Pleistocene clay and gypsum and Middle Eocene marl. Differentiating between such materials with vertical electrical soundings is rather difficult.

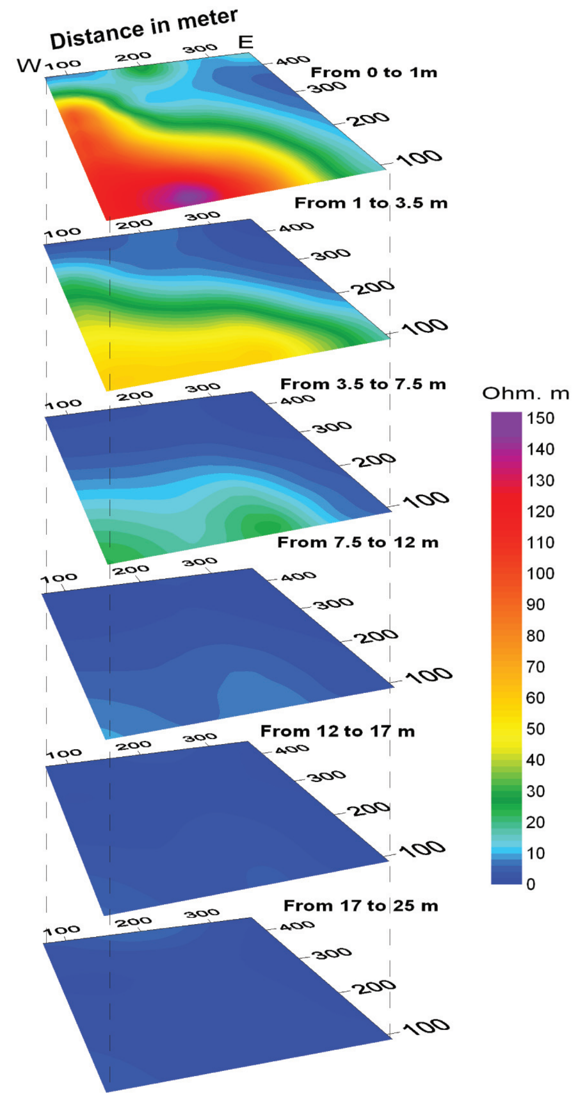

FIGURE 6
3D resistivity model resulting from the inversion of VES.

VERY LOW FREQUENCY-EM

The theoretical basics of VLF-EM, in addition to its geological and hydrogeological applications, can be found in literature, e.g., McNeill and Labson (1991). A low frequency field is sent out from many radio transmitters distributed in different parts of the world, designed for military communications and navigation. The transmitted frequency is usually between 15–30 kHz. At very large distances, these powerful radio transmitters induce electric currents in buried conductive structures. Induced currents produce secondary magnetic fields that can be detected at the surface through deviations of the normal VLF field. The resultant elliptically polarized electromagnetic field consists of two components of the same frequency but of different amplitudes out of phase with each other. The amplitude of the component, which is in-phase with the primary field, is the real or in-phase component while the other component, which is out-of-phase with the primary field, is the imaginary or out-of-phase or quadrature component. Assuming a 2D conductivity distribution, with strike in the x-direction and the y-direction as the measuring profile direction, the VLF-EM instruments measure only the vertical (Hz) and the horizontal (Hy) component of the magnetic field. At each measurement point it is possible to define a scalar tipper B given by $Hz = B\,Hy$. The tipper is a complex quantity originated by the time lag between horizontal and vertical components of the magnetic fields due to the electromagnetic induction phenomena. Over a 2D earth, the tipper varies along the measuring profile showing the strongest variations in the vicinity of resistivity contrasts. The real and imaginary components of the tipper in the case of the VLF-EM method are measured as a percentage of the primary field.

Qualitative interpretation of VLF-EM data

Qualitative interpretation of VLF-EM data is based on filtering procedures. Fraser (1969) and Karous–Hjelt (Karous and Hjelt 1983) filtering are the two methods most widely used in processing VLF-EM data.

Fraser filtering

A Fraser filter is applied to the tilt angle of the magnetic polarization ellipse (real component). The Fraser filter calculates horizontal gradients and smoothes the data to give maximum values over conductors that can then be contoured. Consequently, the plotted Fraser filter function becomes,

$$F2,3 = (M3 + M4) - (M1 + M2), \tag{1}$$

which is plotted midway between the *M*2 and *M*3, tilt angle stations (Fraser 1969).

Accordingly, the Fraser filter: 1) completely removes DC bias and greatly attenuates long wavelength signals; 2) completely removes Nyquist frequency related noise; 3) phase shifts in all frequencies by 90º and (4) has the band-pass centred at a wave length of five times the station spacing. Fraser filtering converts somewhat noisy, non-contourable in-phase components to less noisy, contourable data, which ensures greatly the utility of the VLF-EM survey. VLF-EM contour maps form a meaningful complement to magnetic maps (Sundararajan *et al.* 2006). The Fraser filter transforms the zero-crossing points into peaks, enhancing the signals of the conductive structures. The centre of the anomalous structure may fall directly under the peak of the Fraser filtered data. The seventy five VLF-EM profiles obtained from the application of the Fraser filter to the in-phase data are plotted in a map to show the spatial distribution of the conductive zones (Fig. 7).

After applying the Fraser filter, somewhat elongated and square filtered in-phase VLF-EM anomalies can be observed. They are approximately oriented in the SE-NW and NE-SW directions. These anomalies are produced from alternative positive (good conductors) and negative (bad conductors) peaks. These linear features may be interpreted as the remains of the labyrinth, which was described by Herodotus (II, 148–9): the visitor was guided from courtyards into rooms into galleries into more rooms and from there into more courtyards. Strabo (ca. 64 BC–19 AD) also described the labyrinth as hidden chambers, which are long and large in number and have paths running through one another that twist and turn. However, there are two spikes appearing as strong anomalies in the western side of the area (Fig. 7). They are inadequately disconnected with surrounding weak anomalies. In fact, it is difficult to decide if these are some buried archaeological structures or data errors since they are similar to the anomalous structures in the rest of the map but disconnected with surroundings.

Karous–Hjelt filtering

Another effective filtering technique was proposed by Karous and Hjelt (1977, 1983). It generates an apparent current density pseudosection by filtering the in-phase data. Lower values of relative current density correspond to higher values of resistivity (Benson *et al.* 1997). In the simplest form, the Karous–Hjelt filter is:

$$\left(\frac{\Delta Z}{2\pi}\right) I_a(\Delta x/2) = -0.205H_{-2} + 0.323H_{-1} - 1.446H_0 + 1.446H_1 - 0.323H_2 + 0.205H_3 I_a(x/2) \tag{2}$$

where ΔZ is the assumed thickness of the current sheet, *Ia* is the current density, *x* is the distance between the data points and also

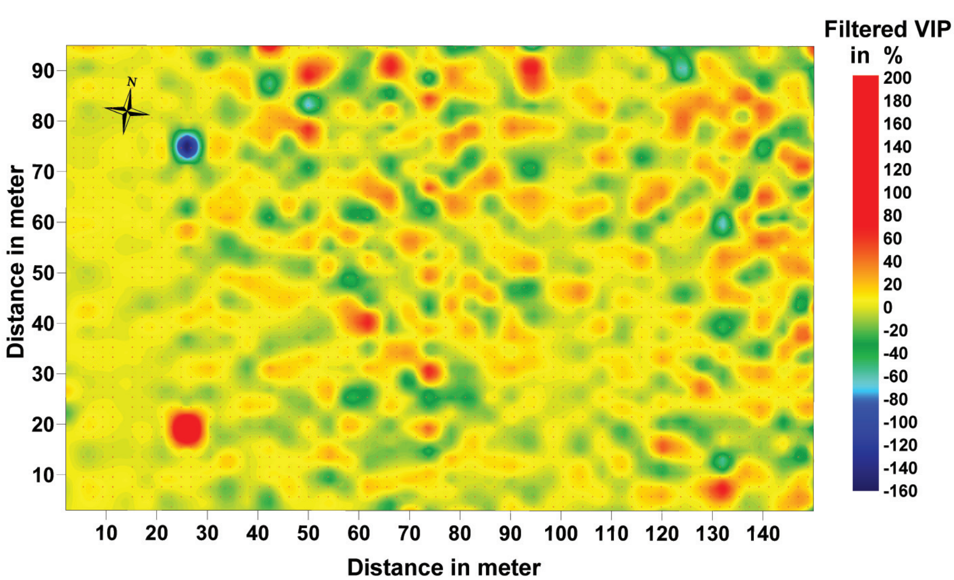

FIGURE 7
Qualitative interpretation of VLF-EM data by a Fraser filter in the form of a contour map (red colour for conductive zones (archaeological remains), soft green for resistive zones (host soil), red points grid is the VLF profiles and stations, scale unit is Fraser filter VLF-in-phase component in per cent).

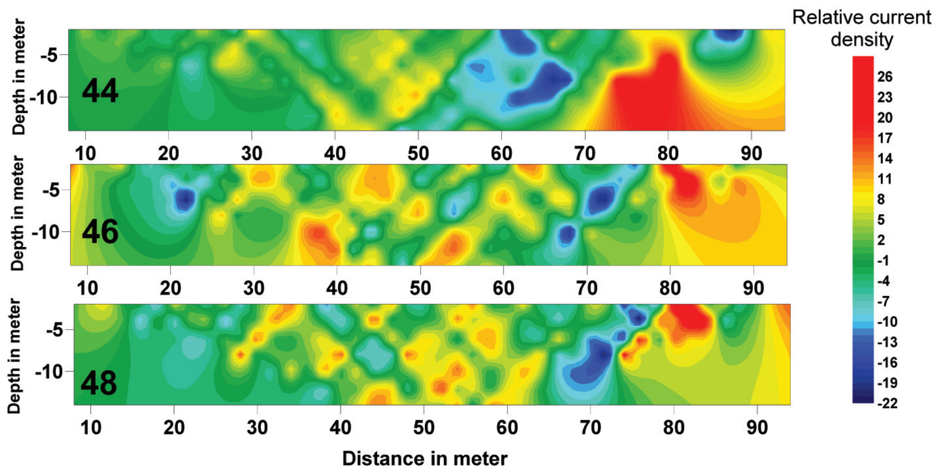

FIGURE 8
Relative current density for three VLF-EM profiles (real component data) calculated using Karous–Hjelt filters.

(a)

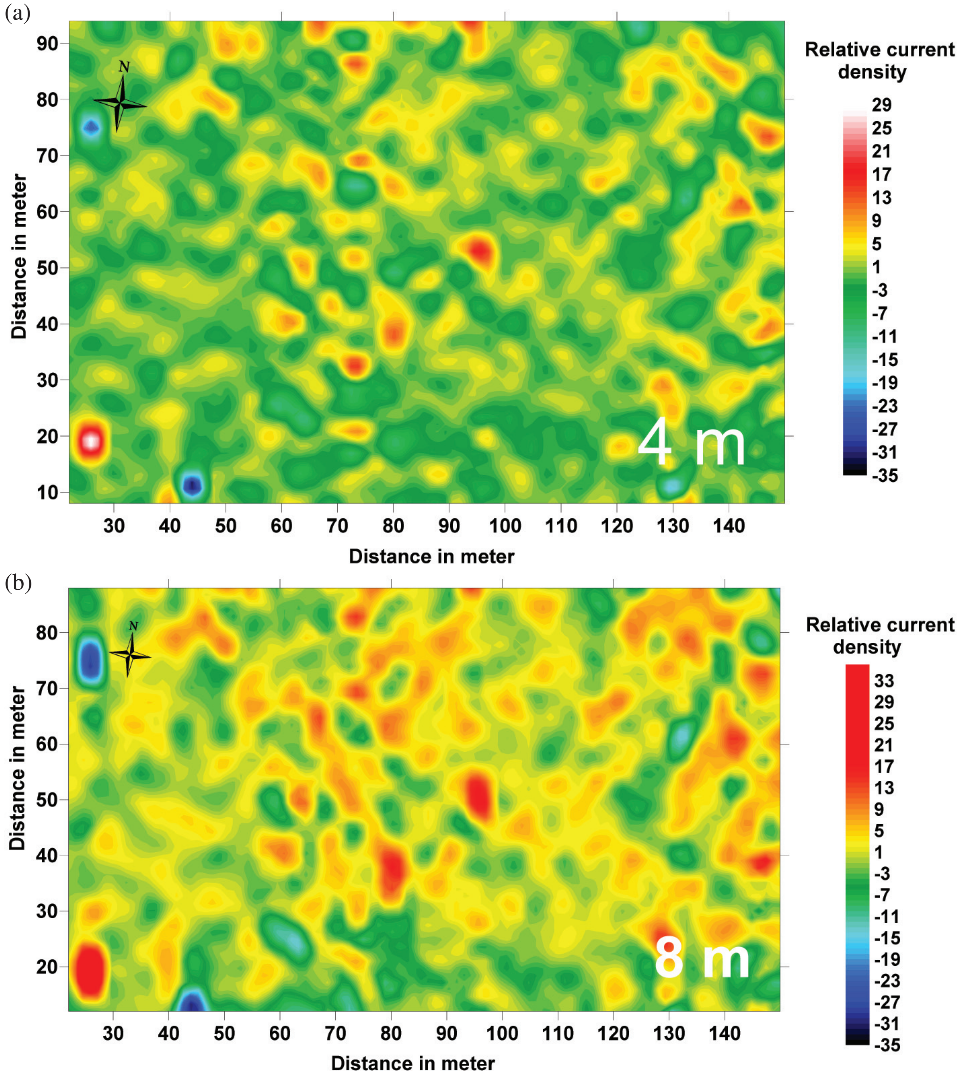

(b)

FIGURE 9
a) Relative current density distribution map calculated using Karous–Hjelt filters, at 4 m depth.
b) Relative current density distribution map calculated using Karous–Hjelt filters, at 8 m depth.

the depth to the current sheet. The values of H_2 through H_3 are the normalized vertical magnetic field anomaly at each of the six data points.

This filter provides a pictorial indication of the depth of the various current concentrations and hence the spatial dispositions of subsurface geological features, such as mineral veins, faults, shear zones and stratigraphic conductors (Ogilvy and Lee 1991). The finite Hjelt filter method is a more generalized and rigorous form of the widely known Fraser filter. However, it is derived directly from the concept of magnetic fields associated with the current flow in the subsurface.

All the seventy five VLF-EM profiles in this study were processed using the Karous–Hjelt filter. The code was prepared by Pirttijärvi (2004). Figure 8 is an example of three successive VLF-profiles numbers 44, 46 and 48. It shows the relative current density (real component data) calculated using Karous-Hjelt filters. The positive contour values (yellow and red ones) correspond to the areas of high current density flow, which is corresponding to high conductive anomalies. On the other side, negative contours are due to high resistivities. From the figure it is easy to pursue the horizontal extension of high conductive zones but regarding seventy five VLF profiles, it will be very difficult to track the horizontal distribution and extension of all anomalies over the entire study area. However, contour maps at different depths were prepared for this purpose. Depths of 4 m and 8 m are selected to illustrate the results (Fig. 9a,b).

Matching between outcomes of the Karous–Hjelt filter and Fraser filter indicates a fairly good agreement in the anomaly positions. In the Karous–Hjelt filter, linear features are disseminated and disconnected at 4 m depth, while at 8 m, they are connected. This may indicate that the reasonable depth of future excavation should be more than 4 m deep.

Quantitative interpretation

A quantitative interpretation of single frequency VLF-EM data was carried out via inversion of the tipper data using the 2D regularized inversion approach based on Sasaki (1989, 2001). We used Inv2DVLF software developed by Monteiro Santos *et al.* (2006). This code for 2D regularized inversion of VLF-EM data was developed based on a forward solution using the finite-element method. The same theoretical bases and inversion method used previously in resistivity interpretation are used in this section but in 2D approach. The objective of the inversion is to obtain a subsurface distribution of the electrical resistivity, which generates a response that fits the field data within the limits of data errors.

Tipper data (real and imaginary components) of the measured VLF-EM profiles have been interpreted using the Inv2DVLF software. A 20 Ωm uniform half-space was used as an initial model.

Twenty iterations were found to be reasonable to get an acceptable global misfit, which ranges in the majority of VLF profiles from 1–5% but seldom reaches 12%.

The resulting 2D resistivity cross-sections are all combined, according to their individual relative coordinates and a 3D view of the resistivity models was constructed and presented in the form of horizontal depth slices. Figure 10 illustrates the vertical and horizontal resistivity distribution at different depths, from the surface to 12 m depth. The slices show a very high resistivity zone in the northern part of the study area, extending to a depth of 5 m, which may correspond to the shallow high resistive Pleistocene sands and gravels. The other parts of the study area

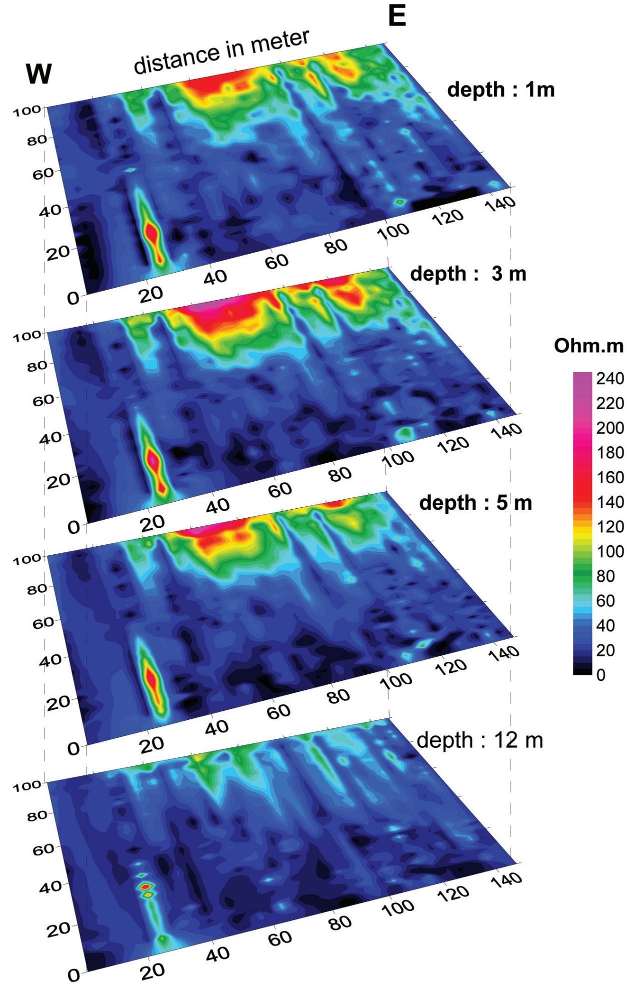

FIGURE 10
Iso-resistivity maps at different depths obtained from the results of 2D inversion.

comprise middle to very low resistivity values ranging from 45–1 Ωm. The obvious contrast between middle resistivity values and very low ones at depths of 3 m, 5 m and 12 m, which form linear and square features, may refer to the remains of archaeological parts. Especially, they are in the same range of depth detected by the Karous–Hjelt filter (Fig. 9a,b).

CONCLUSION

The very low frequency electromagnetic method (VLF-EM) was applied to check the historical legend about the shape and structure of the labyrinth mortuary temple complex, which is located south of the Hawara pyramid. The VLF data were supplemented by vertical electrical soundings (VES).

Seventy five VLF-EM profiles were measured in a relatively small grid in the area of the labyrinth. The VLF-real data (in-phase) were processed and interpreted by the Fraser filter. The result shows spatially distributed elongated and square shaped

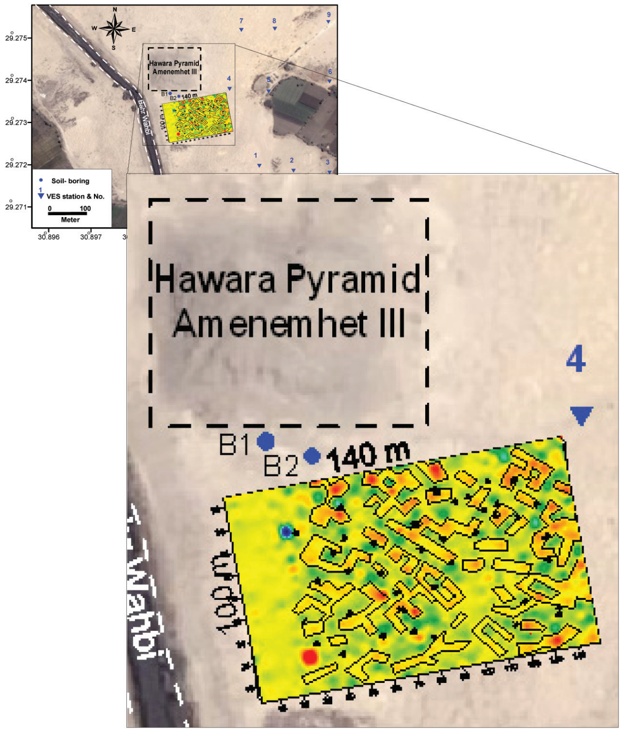

FIGURE 11
The main result of the study in the framework of an archaeological site showing the complex of the labyrinth mortuary temple.

subsurface anomalies, which may identify the walls and rooms of the labyrinth mortuary temple complex. Similar spatial distribution of such anomalies was outlined by application of the Karous-Hjelt filter, particularly at 8 m depth.

2D resistivity inversion of the VLF-EM data in the form of horizontal slices showed a contrast between intermediate and very low resistivity values at depths of 3 m, 5 m and 12 m. There are elongated structure features that may correspond to parts of the labyrinth mortuary temple complex that are in the same range of depth as those detected by the Karous–Hjelt filter. The VLF-EM technique showed a fairly good result as a means of archaeological prospecting, as seen from Fig. 11 that outlines the expected shape and structure of the archaeological remains of the labyrinth mortuary temple complex, based on the different techniques used in the present survey.

The resulting vertical resistivity distribution from the 3D inversion of VES data is in the same range as that resulting from 2D resistivity inversion of VLF-EM data, matching well with the shallow geologic information. Inverted models of the VLF-EM and VES data are in agreement with respect to the general resistivity structure of the area. Anomalies were observed in the VLF-EM data that may be originated from remains of the labyrinth. However, no alternative information is available to support the present interpretation. Nevertheless, we hope the site may be excavated in the future based on these survey results.

ACKNOWLEDGEMENTS

The main author is indebted to the Fundação para a Ciência e Tecnologia (Portugal) for his support through the post-doctoral fellowship (SFRH\BPD\29971/2006). This work was partly developed in the scope of the scientific cooperation agreement between the CGUL and the NRIAG. The authors also express their thanks to Mark Beaver and Louis De Cordier for their help to conduct the work. We also acknowledge Ghent University for the logistical support. We are truly grateful to E. Ramalho and D. Oliveira for improving the English version of the manuscript. Thanks are also due to the anonymous referees, whose reviews, comments and suggestions contributed to improve this paper.

REFERENCES

Armayor O.K. 1985. *Herodotus's Autopsy of the Fayoum: Lake Moeris and the Labyrinth of Egypt*. Amsterdam.

Arnold D. 1979. Das Labyrinth und seine Vorbilder. *Mitteilungen des Deutschen Archäologischen Institus Kairo* **35**, 1–9.

Benson A.K., Payne K.L. and Stubben M.A. 1997. Mapping groundwater contamination using dc resistivity and VLF geophysical methods – A case study. *Geophysics* **62**, 80–86.

Bozzo E., Merlanti F., Ranieri G., Sambuelli L. and Finzi E. 1999. EM-VLF soundings on the Eastern Hill of the archaeological site of Selinunte. *Bollettino di Geofisica Teorica ed Applicata* **34**, 169–180.

Brown R.H. 1892. *The Fayum and Lake Moeris*. E. Stanford, London.

Broyden 1965. A class of methods for solving nonlinear simultaneous equations. *Mathematics of Computation* **19**, 577–593.

Butzer K.W. 1976. *Early Hydraulic Civilization in Egypt: A Study in Cultural Ecology*. University of Chicago Press.

Fraser D.C. 1969. Contouring of VLF-EM data. *Geophysics* **34**, 958–967.

Herodotus. ca. 484–430 BC. *One Passage in Histories*. Book, II, 148.

Jomard E. and Caristie A.N. 1822. Description des ruines situées près de la pyramide de Haouârah, considerées comme les restes du labyrinthe, en comparaison de ces ruines avec les récits des anciens. In: *Description de la Égypte, ou recueil des observations et des recherches qui ont été faites en Égypte pendant l'expédition de l'armée française* (ed. C.L.F. Panckoucke).

Karous M. and Hjelt S.E. 1977. Determination of apparent current density from VLF measurements. Report, Department of Geophysics, University of Oulu, Finland, Contribution no. 89.

Karous M. and Hjelt S.E. 1983. Linear filtering of VLF dip-angle measurements. *Geophysical Prospecting* **31**, 782–794.

Keatings K., Tassie G.J., Flower R.J., Hassan F.A., Hamdan M.A.R., Hughes M. and Arrowsmith C. 2007. An examination of groundwater within the Hawara Pyramid, Egypt. *Geoarchaeology: An International Journal* **22**, 533–554.

Kern H. 1995. *Labyrinth*. Prestel-Verlag, Munich.

Lepsius R. 1849. *Denkmaler aus Ägypten und Äthiopten.* II, 11-30. Berlin.

Lloyd A.B. 1970. The Egyptian labyrinth. *Journal of Egyptian Archaeology* **56**, 81–100.

Loke M.H. and Barker R.D. 1996. Rapid least-squares inversion of apparent resistivity pseudosections by a quasi-Newton method. *Geophysical Prospecting* **44**, 131–152.

Mahmut G.D. 2006. Integrated geophysical studies in the upper part of Sardis archaeological site, Turkey. *Journal of Applied Geophysics* **59**, 205–223.

McNeill J.D. and Labson V.F. 1991. Geological mapping using VLF radio fields. In: *Electromagnetic Methods in Applied Geophysics II* (ed. M.N. Nabighian), pp. 521–640. SEG.

Monteiro Santos F.A., Mateus A., Figueiras J. and Gonçalves M.A. 2006. Mapping groundwater contamination around a landfill facility using the VLF-EM method – A case study. *Journal of Applied Geophysics* **60**, 115–125.

Monteiro Santos F.A. and Sultan S.A. 2008. On the 3-D inversion of Vertical Electrical Soundings: application to the South Ismailia area, Cairo Desert Road, Cairo, Egypt. *Journal of Applied Geophysics* **65**, 97–110.

Ogilvy R.D. and Lee A.C.1991. Interpretation of VLF-EM inphase data using current density pseudosections. *Geophysical Prospecting* **39**, 567–580.

Papadopoulos N.G., Tsourlos P., Tsokas G.N. and Sarris A. 2007. Efficient ERT measuring and inversion strategies for 3D imaging of buried antiquities. *Near Surface Geophysics* **5**, 349–362.

Petrie W.M.F. 1889. *Hawara, Biahmu and Arsinoe*. Field & Tuer, London.

Petrie W.M.F. 1890. *Kahun, Gurob and Hawara*. Field & Tuer, London.

Petrie W.M.F., Wainwright G.A. and Mackay E. 1912. *The Labyrinth, Gerzeh and Mazghuneh* (British School of Archaeology in Egypt and Egyptian Research Account, 18th Year). Bernard Quaritch, London.

Pirttijärvi M. 2004. Karous–Hjelt and Fraser filtering of VLF measurements. Manual of the KHFFILT Program.

Pliny. 23–79 AD. *One Passage in His Natural History*. Book 36, 13.

Sasaki Y. 1989. Two-dimensional joint inversion of magnetotelluric and dipole–dipole resistivity data. *Geophysics* **54**, 254–262.

Sasaki Y. 1994. 3-D resistivity inversion using the finite element method. *Geophysics* **59**, 1839–1848.

Sasaki Y. 2001. Full 3-D inversion of electromagnetic data on PC. *Journal of Applied Geophysics* **46**, 45–54.

Strabo. ca. 64 BC–19 AD. *Three Passages in his Geography*. Book 17, I, 3 and 37 and 42.

Sundararajan N, Ramesh Babub V., Shiva Prasadb N. and Srinivas Y. 2006. VLFPROS – A Matlab code for processing of VLF-EM data. *Computers and Geosciences* **32**, 1806–1813.

Swedan A.H. 1986. *Contributions to the geology of Fayoum area*. PhD thesis, Faculty of Science, Cairo University.